PERGAMON

International Journal of Solids and Structures 39 (2002) 199–212

INTERNATIONAL JOURNAL OF SOLIDS and STRUCTURES

www.elsevier.com/locate/ijsolstr

Apparent elastic and elastoplastic behavior of periodic composites

M. Jiang [a], I. Jasiuk [b,*], M. Ostoja-Starzewski [c]

[a] *General Electric Corporate R&D, 1 Research Circle, Bldg. KW, Rm. C1610, Niskayuna, NY 12309, USA*
[b] *The George W. Woodruff School of Mechanical Engineering, Georgia Institute of Technology, Atlanta, GA 30332-0405, USA*
[c] *Department of Mechanical Engineering, McGill University, Montreal, Quebec H3A 2K6, Canada*

Received 10 August 2000; in revised form 31 May 2001

Abstract

We investigate scale and boundary conditions effects on the elastic and elastoplastic behavior of periodic fiber-reinforced composites. Four boundary conditions, including displacement controlled, traction controlled, mixed (normal displacements and zero shear tractions specified on each boundary) and periodic boundary conditions, are considered. Influence of several factors – such as the window size, the mismatch between component phases' properties, and the types of boundary conditions – on the apparent mechanical response (elastic and elastoplastic) is studied. It is shown that the apparent properties obtained under our mixed and periodic conditions are the same within numerical accuracy, and they are bounded by those obtained using displacement and traction controlled boundary conditions. From our study of elastic case, it is found that the bounds are very sensitive to the mismatch of phase moduli: the higher the mismatch, the wider are the bounds. In the study of elastoplastic case, monotonically increasing proportional loading is applied to different sized windows under each of the above four boundary conditions. An explanation of response curves can be reached through the observation of shear bands, under these various boundary conditions.

Keywords: Elasticity; Elastoplasticity; Scale and boundary conditions effects; Fiber-reinforced composite materials; Energy methods; Finite elements; Periodic microstructures

1. Introduction

Conventional mechanics of materials is, to a large extent, based on the concepts of representative volume element (RVE) and effective property. Mathematically, the RVE is an infinite length scale limit, relative to the microscale (or the length scale of a single heterogeneity), in which the material appears uniform and the

* Corresponding author. Tel.: +1-404-894-6597; fax: +1-404-894-0186.
E-mail address: iwona.jasiuk@me.gatech.edu (I. Jasiuk).

0020-7683/01/$ - see front matter
PII: S0020-7683(01)00145-7

continuum concept may be applied. It is well known that, thanks to this uniform setting, the methods of analysis, especially with respect to boundary value problems, can successfully be applied.

For example, the deterministic finite element method relies on the homogeneous continuum assumption with regard to every element within the mesh. However, many problems in mechanics of materials require a careful consideration of dependent fields over scales not infinitely larger than the microscale. The postulated RVE concept, which requires elements to be much larger than a single heterogeneity, can hardly be used and a study of properties of a finite size domain is necessary.

When referring to the finite size domain of material the term apparent property is used (Huet, 1990). The term effective is reserved for the overall response of RVE, which is infinite compared to a single fiber dimension. The dependence of apparent properties on the window size and boundary conditions applied is referred to as coupled scale and boundary conditions effects. The quantitative dependence of apparent properties on these and other factors, such as the mismatch of phases' properties, volume fractions, geometric information of microstructures, is impossible to obtain by purely analytical methods and was mainly investigated numerically for linear elastic periodic composites (e.g., Hollister and Kikuchi, 1992; Pecullan et al., 1999) and for linear elastic random materials (e.g., Ostoja-Starzewski, 1993, 1998, 1999).

Little work has been done on the topic of scale and boundary conditions effects of nonlinear heterogeneous materials even though the research on the nonlinear effective response of heterogeneous materials has actively been carried out both theoretically (e.g., Accorsi and Nemat-Nasser, 1986; Gibiansky and Torquato, 1998; Ponte Castañeda, 1992; Ponte Castañeda and Suquet, 1998; Talbot and Willis, 1985, 1998) and numerically (e.g., Brockenbrough et al., 1991; Shen et al., 1995; Werwer et al., 1998). Assuming the form of constitutive law employed by Kröner (1994), Hazanov (1999) showed that the effective response of a nonlinear elastic heterogeneous material is bounded by ensemble average responses of finite size domain of material under displacement controlled and traction controlled boundary conditions. Jiang et al. (2001a) extended this result to elastoplastic materials under proportional loading.

In this paper we carry out an investigation of scale and boundary conditions effects on the elastic and elastoplastic behavior of a two-dimensional (2D) periodic fiber-reinforced composite with circular inclusions arranged in a triangular (equilateral) array. More specifically, we consider the case of long cylindrical fibers with circular cross-sections. Such geometry represents a transverse plane of a unidirectional fiber-reinforced composite, the deformation being of plane strain type. The boundary conditions considered are displacement controlled, traction controlled, periodic and a special kind of mixed boundary condition, in which normal displacements and zero shear tractions are specified on each boundary.

The outline of the paper is as follows. Following the problem statement, we review the hierarchy structure of nonlinear elastic properties. This result can also be used in the elastoplastic response analysis under a monotonically increasing proportional loading. In this situation, the elastoplastic response can be treated in the framework of deformation theory, which is formally equivalent to the physically nonlinear, small-deformation elasticity. We then investigate numerically the effects of scale, boundary conditions, and material mismatch on apparent elastic and elastoplastic properties of fiber-reinforced composite. It is shown that the responses under the periodic boundary condition and the mixed boundary condition (normal displacement and zero shear tractions specified on the boundary) are the same within numerical accuracy for the loadings considered, and they are bounded by those under displacement and traction controlled boundary conditions. In general, the differences between responses under various boundary conditions become smaller as the window size increases.

Our paper extends earlier studies of apparent elastic properties of periodic composites (e.g., Hollister and Kikuchi, 1992; Pecullan et al., 1999). We consider additional boundary conditions and conduct both elastic and elastoplastic analyses.

2. Theoretical background

We consider periodic composite materials characterized by one microscale, i.e., the diameter $d\ (=2r)$ of fibers (see Fig. 1). The fibers are arranged in an equilateral triangular array. We assume that both matrix and fibers are isotropic; fibers are elastic, while the matrix is either elastic or elastoplastic. The interface between each fiber and the matrix is perfectly bonded. All the fibers are continuous and aligned, so that our problem is one of plane strain in the x_1, x_2-plane. We obtain transverse elastic and elastoplastic responses of this composite under several types of boundary conditions applied to finite sized domains of material; such a domain is called a window (Ostoja-Starzewski, 1993). The smallest window, a unit cell, is shown in Fig. 1. We define the unit cell in Fig. 1 to be of scale δ_0. We use $\delta = n\delta_0$ to represent a larger window whose size is n times δ_0 in both x_1 and x_2 directions. The window of size δ is denoted as B_δ, and its boundary is ∂B_δ.

It is known that the Hill condition, $\overline{\boldsymbol{\sigma} : \boldsymbol{\varepsilon}} = \overline{\boldsymbol{\sigma}} : \overline{\boldsymbol{\varepsilon}}$ is the necessary and sufficient condition for the equivalence of energetically and mechanically defined apparent properties of heterogenous linear elastic materials (Huet, 1990); $\boldsymbol{\sigma}$ and $\boldsymbol{\varepsilon}$ are the stress and strain tensors, respectively, and we use an overbar to denote a volume average.

The Hill condition for nonlinear heterogeneous materials, in a static case, was given by Hazanov (1998, 1999)

$$\overline{\int \boldsymbol{\sigma} : \mathrm{d}\boldsymbol{\varepsilon}} = \int \overline{\boldsymbol{\sigma}} : \mathrm{d}\overline{\boldsymbol{\varepsilon}} \tag{2.1}$$

It is equivalent to

$$\int_{\partial B_\delta} (\boldsymbol{t} - \overline{\boldsymbol{\sigma}} \cdot \boldsymbol{n}) \cdot \mathrm{d}(\boldsymbol{u} - \overline{\boldsymbol{\varepsilon}} \cdot \boldsymbol{x})\, \mathrm{d}S = 0 \tag{2.2}$$

From Eq. (2.2), one can obtain three kinds of boundary conditions. They are

Kinematic uniform boundary condition (or displacement controlled boundary condition, dd)

$$\boldsymbol{u} = \overline{\boldsymbol{\varepsilon}} \cdot \boldsymbol{x}, \quad \forall \boldsymbol{x} \in \partial B_\delta \tag{2.3}$$

Static uniform boundary condition (or traction controlled boundary condition, tt)

$$\boldsymbol{t} = \overline{\boldsymbol{\sigma}} \cdot \boldsymbol{n}, \quad \forall \boldsymbol{x} \in \partial B_\delta \tag{2.4}$$

Mixed uniform boundary condition (dt)

$$(\boldsymbol{t} - \overline{\boldsymbol{\sigma}} \cdot \boldsymbol{n}) \cdot (\boldsymbol{u} - \overline{\boldsymbol{\varepsilon}} \cdot \boldsymbol{x}) = 0, \quad \forall \boldsymbol{x} \in \partial B_\delta \tag{2.5}$$

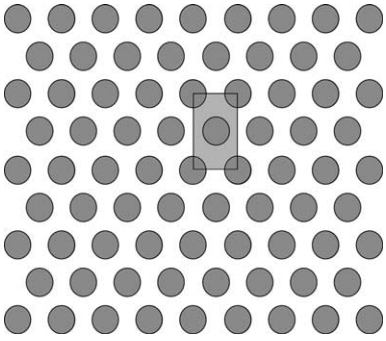

Fig. 1. Periodic composite and a unit cell.

Besides the above boundary conditions, we also use periodic boundary condition (pp), i.e.,

$$\boldsymbol{u}(\boldsymbol{x}+\boldsymbol{L}) = \boldsymbol{u}(\boldsymbol{x}) + \overline{\boldsymbol{\varepsilon}} \cdot \boldsymbol{L}, \qquad \boldsymbol{t}(\boldsymbol{x}+\boldsymbol{L}) = -\boldsymbol{t}(\boldsymbol{x}), \quad \forall \boldsymbol{x} \in \partial B_\delta \tag{2.6}$$

We use the strain and stress averaging theorems

$$\overline{\boldsymbol{\varepsilon}} = \boldsymbol{\varepsilon}^0, \quad \overline{\boldsymbol{\sigma}} = \boldsymbol{\sigma}^0 \tag{2.7}$$

where $\boldsymbol{\varepsilon}^0$ and $\boldsymbol{\sigma}^0$ are uniform applied strain and stress tensors. Recall the classical fact that the strain averaging theorem requires the assumption of perfectly bonded fiber–matrix interfaces. Thus, alternately, we can write the conditions (2.3) and (2.4) as

$$\boldsymbol{u} = \boldsymbol{\varepsilon}^0 \cdot \boldsymbol{x}, \quad \boldsymbol{t} = \boldsymbol{\sigma}^0 \cdot \boldsymbol{n} \tag{2.8}$$

It was first proved by Huet (1990) that the linear effective elastic stiffness is bounded by apparent properties obtained under displacement and traction boundary conditions. Following the same approach, for a nonlinear elastic heterogeneous material, in (Jiang et al., 2001a), we found

$$w^{\text{eff}}(\boldsymbol{\varepsilon}^0) < w(\boldsymbol{\varepsilon}^0, n\delta_0) < w(\boldsymbol{\varepsilon}^0, n'\delta_0) < w(\boldsymbol{\varepsilon}^0, \delta_0) < w^{\text{V}}(\boldsymbol{\varepsilon}^0) \quad \forall 1 < n' < n \tag{2.9}$$

and

$$w^{*\text{eff}}(\boldsymbol{\sigma}^0) < w^*(\boldsymbol{\sigma}^0, n\delta_0) < w^*(\boldsymbol{\sigma}^0, n'\delta_0) < w^*(\boldsymbol{\sigma}^0, \delta_0) < w^{*\text{R}}(\boldsymbol{\sigma}^0) \quad \forall 1 < n' < n \tag{2.10}$$

with $w(\boldsymbol{\varepsilon}^0, n\delta_0)$ and $w^*(\boldsymbol{\sigma}^0, n\delta_0)$ representing the volume average strain energy density and the volume average complementary energy density functions under displacement and traction boundary conditions, respectively, of a window of size $\delta = n\delta_0$. $w^{\text{V}}(\boldsymbol{\varepsilon}^0)$ and $w^{*\text{R}}(\boldsymbol{\sigma}^0)$ stand for, respectively, the quantities obtained under Voigt assumption (strain is uniform everywhere in the material) and Reuss assumption (stress is uniform everywhere in the material).

It is known that the effective elastoplasticity under proportional loading can be investigated within a framework of effective nonlinear elasticity. For example, the problem of an isotropic physically nonlinear incompressible elastic material is equivalent to the J_2-deformation theory of plasticity. In this case, following (Ponte Castañeda and Suquet, 1998), the strain energy density and complementary energy density can be written as

$$w(\boldsymbol{\varepsilon}) = \varphi(\varepsilon_{\text{eq}}) \tag{2.11}$$

and

$$w^*(\boldsymbol{\sigma}) = \psi(\sigma_{\text{eq}}) \tag{2.12}$$

where φ and ψ are dual convex potentials of a scalar variable. σ_{eq} and ε_{eq} are the von Mises effective stress and effective strain, respectively

$$\sigma_{\text{eq}} = \left(\tfrac{3}{2}\boldsymbol{\sigma}_{\text{d}} : \boldsymbol{\sigma}_{\text{d}}\right)^{1/2}, \qquad \varepsilon_{\text{eq}} = \left(\tfrac{3}{2}\boldsymbol{\varepsilon}_{\text{d}} : \boldsymbol{\varepsilon}_{\text{d}}\right)^{1/2} \tag{2.13}$$

$\boldsymbol{\sigma}_{\text{d}}$ and $\boldsymbol{\varepsilon}_{\text{d}}$ are the deviatoric stress and strain, respectively

$$\boldsymbol{\sigma}_{\text{d}} = \boldsymbol{\sigma} - \sigma_{\text{m}}\boldsymbol{I}, \qquad \boldsymbol{\varepsilon}_{\text{d}} = \boldsymbol{\varepsilon} - \varepsilon_{\text{m}}\boldsymbol{I} \tag{2.14}$$

where σ_{m} and ε_{m} are the hydrostatic stress and strain

$$\sigma_{\text{m}} = \tfrac{1}{3}\text{tr}(\boldsymbol{\sigma}), \qquad \varepsilon_{\text{m}} = \tfrac{1}{3}\text{tr}(\boldsymbol{\varepsilon}) \tag{2.15}$$

The resulting stress–strain relations can be written as

$$\boldsymbol{\sigma}_{\text{d}} = 2\mu(\varepsilon_{\text{eq}})\boldsymbol{\varepsilon}_{\text{d}} \tag{2.16}$$

where

$$\mu(\varepsilon_{\mathrm{eq}}) = \frac{\sigma_{\mathrm{eq}}}{3\varepsilon_{\mathrm{eq}}} = \frac{\varphi'(\varepsilon_{\mathrm{eq}})}{3\varepsilon_{\mathrm{eq}}} = \frac{\sigma_{\mathrm{eq}}}{3\psi'(\sigma_{\mathrm{eq}})} \tag{2.17}$$

The Ramberg–Osgood model in the J_2-deformation theory of plasticity corresponds to the choice

$$\psi(\sigma_{\mathrm{eq}}) = \frac{1}{6\mu_0}\sigma_{\mathrm{eq}}^2 + \frac{\sigma_0\varepsilon_0}{n+1}\left(\frac{\sigma_{\mathrm{eq}}}{\sigma_0}\right)^{n+1} \tag{2.18}$$

where μ_0 is the initial elastic shear modulus, σ_0 is the yield stress, ε_0 is the yield strain, $n \geqslant 1$ is the hardening exponent, and prime denotes a derivative.

In our work, we go one step further with the following assumption: for a heterogeneous material, the investigation of apparent elastoplastic response, under proportional monotonically increasing loading, can also be treated within the framework of deformation theory, which is formally equivalent to a physically nonlinear, small-deformation elasticity theory.

When the material is linear elastic, we have

$$w(\boldsymbol{\varepsilon}^0, n\delta_0) = \tfrac{1}{2}\boldsymbol{\varepsilon}^0 : \boldsymbol{C}^{\mathrm{dd}}_{n\delta_0} : \boldsymbol{\varepsilon}^0, \qquad w^*(\boldsymbol{\sigma}^0, n\delta_0) = \tfrac{1}{2}\boldsymbol{\sigma}^0 : \boldsymbol{S}^{\mathrm{tt}}_{n\delta_0} : \boldsymbol{\sigma}^0 \tag{2.19}$$

for apparent properties, using boundary conditions (2.3) and (2.4), respectively, and

$$w^{\mathrm{eff}} = \tfrac{1}{2}\boldsymbol{\varepsilon}^0 : \boldsymbol{C}^{\mathrm{eff}} : \boldsymbol{\varepsilon}^0, \qquad w^{*\mathrm{eff}} = \tfrac{1}{2}\boldsymbol{\sigma}^0 : \boldsymbol{S}^{\mathrm{eff}} : \boldsymbol{\sigma}^0 \tag{2.20}$$

for effective properties. In Eq. (2.19) the superscripts dd and tt denote displacement and traction boundary conditions, respectively, and the subscript $n\delta_0$ indicates the apparent property of a window of size $n\delta_0$. Because of $(\boldsymbol{S}^{\mathrm{eff}})^{-1} = \boldsymbol{C}^{\mathrm{eff}}$, Eqs. (2.9) and (2.10) can be reduced to

$$\boldsymbol{C}^{\mathrm{R}} \equiv (\boldsymbol{S}^{\mathrm{R}})^{-1} < (\boldsymbol{S}^{\mathrm{tt}}_{\delta_0})^{-1} < (\boldsymbol{S}^{\mathrm{tt}}_{n'\delta_0})^{-1} < (\boldsymbol{S}^{\mathrm{tt}}_{n\delta_0})^{-1} < \boldsymbol{C}^{\mathrm{eff}} < \boldsymbol{C}^{\mathrm{dd}}_{n\delta_0} < \boldsymbol{C}^{\mathrm{dd}}_{n'\delta_0} < \boldsymbol{C}^{\mathrm{dd}}_{\delta_0} < \boldsymbol{C}^{\mathrm{V}}, \quad \forall 1 < n' < n \tag{2.21}$$

which is the structure obtained by Huet (1990) and Ostoja-Starzewski (1993). The comparison of tensors is understood in terms of quadratic forms. This means that for two fourth rank tensors $\boldsymbol{C}$ and $\boldsymbol{D}$, the assumption $\boldsymbol{C} > \boldsymbol{D}$ implies that

$$(\boldsymbol{C} - \boldsymbol{D}) : \boldsymbol{a} : \boldsymbol{a} > 0 \quad \text{for any tensor} \quad \boldsymbol{a} \neq 0 \tag{2.22}$$

The linear apparent elastic property under mixed boundary conditions was first discussed by Hazanov and Huet (1994) and Hazanov and Amieur (1995). They proved that, for any given window,

$$\boldsymbol{C}^{\mathrm{tt}} < \boldsymbol{C}^{\mathrm{dt}} < \boldsymbol{C}^{\mathrm{dd}}, \qquad \boldsymbol{S}^{\mathrm{dd}} < \boldsymbol{S}^{\mathrm{dt}} < \boldsymbol{S}^{\mathrm{tt}} \tag{2.23}$$

In the next section, we also choose a special mixed boundary loading, under which we investigate the elastic and elastoplastic response.

3. Apparent elastic properties

We assume both matrix and fibers to be linearly elastic and isotropic. For a fiber-matrix composite with triangular packing, the apparent elastic tensor of a window, with size $n\delta_0$, is orthotropic. The apparent tensor can be represented by

$$\boldsymbol{C}^{\text{app}} = \begin{bmatrix} C_{1111} & C_{1122} & 0 \\ C_{1122} & C_{2222} & 0 \\ 0 & 0 & C_{1212} \end{bmatrix} \tag{3.1}$$

with $C_{1111} \neq C_{2222}$. The orthotropy becomes weaker as the window size increases. When the window becomes infinite (RVE size), the apparent elastic tensor will coincide with the effective one, which is isotropic for a triangularly arranged fiber-reinforced composite.

We use a finite element analysis (FEA) to investigate the apparent properties. Two loadings for all four kinds of boundary conditions (dd, dt, tt, pp) are used to investigate the apparent properties of a given window:

Loading (1): Uniform in-plane all-around extension, corresponding to a macroscopic strain $\varepsilon^0_{11} = \varepsilon^0_{22} = \varepsilon^0$ (or $\sigma^0_{11} = \sigma^0_{22} = \sigma^0$); we calculate the total energy $U_{(1)}$ as a sum of energies of all elements in the window.

Loading (2): Uniform extension in x_1 direction and a uniform compression in x_2 direction, $\varepsilon^0_{11} = -\varepsilon^0_{22} = \varepsilon^0$ (or $\sigma^0_{11} = -\sigma^0_{22} = \sigma^0$), corresponding to a shear strain $\varepsilon^0_{12} = \varepsilon^0$ (or shear stress $\sigma^0_{12} = \sigma^0$) in a coordinate system rotated by $\pi/4$ for an effectively homogeneous material. We then calculate the total energy $U_{(2)}$ as a sum of energies of all elements in the window.

Under the periodic boundary condition (Eq. (2.6)) applied on the unit cell shown in Fig. 1, the obtained apparent properties are just the effective ones, i.e., isotropic. We obtain the effective bulk and shear moduli, respectively, as

$$K^{\text{eff}} = \frac{U_{(1)}}{2V(\varepsilon^0)^2} \quad \text{and} \quad \mu^{\text{eff}} = \frac{U_{(2)}}{2V(\varepsilon^0)^2} \tag{3.2}$$

Under the displacement (dd) boundary condition, we apply Eq. (2.3) with $\varepsilon^0_{11} = \varepsilon^0_{22} = 1$ and $\varepsilon^0_{12} = 0$ to obtain $U_{(1)}$, and Eq. (2.4) with $\varepsilon^0_{11} = -\varepsilon^0_{22} = 1$ and $\varepsilon^0_{12} = 0$ to obtain $U_{(2)}$. Under the mixed (dt) boundary condition, we apply Eq. (2.5) with $\varepsilon^0_{11} = \varepsilon^0_{22} = 1$ and $\sigma^0_{12} = 0$ to obtain $U_{(1)}$, and Eq. (2.5) with $\varepsilon^0_{11} = -\varepsilon^0_{22} = 1$ and $\sigma^0_{12} = 0$ to obtain $U_{(2)}$. We use value 1 for applied strains to simplify the algebra in this linear elastic problem. In order to study the convergence rate of the apparent properties to the effective ones, under displacement or mixed boundary conditions, we define the following apparent bulk and shear moduli (corresponding to the effective isotropic counterparts, with $\varepsilon^0 = 1$ in Eq. (3.2))

$$K^{\text{app}} = \frac{U_{(1)}}{2V} \quad \text{and} \quad \mu^{\text{app}} = \frac{U_{(2)}}{2V}, \quad \text{under dd and dt} \tag{3.3}$$

Under the traction (tt) boundary condition, we use Eq. (3.4) to define the apparent bulk compliance A^{app}_δ and shear compliance χ^{app}_δ with ($\sigma^0_{11} = \sigma^0_{22} = 1$, $\sigma^0_{12} = 0$ in Eq. (2.4)) and ($\sigma^0_{11} = -\sigma^0_{22} = 1$, $\sigma^0_{12} = 0$ in Eq. (2.4)), respectively,

$$A^{\text{app}} = \frac{2U_{(1)}}{V} \quad \text{and} \quad \chi^{\text{app}} = \frac{2U_{(2)}}{V}, \quad \text{under tt} \tag{3.4}$$

The inequality (2.21) means that, when $\delta' < \delta$, we have $(\boldsymbol{C}^{\text{dd}}_{\delta'} - \boldsymbol{C}^{\text{dd}}_{\delta})$:$\boldsymbol{\varepsilon}$:$\boldsymbol{\varepsilon} > 0$ and $(\boldsymbol{S}^{\text{tt}}_{\delta'} - \boldsymbol{S}^{\text{tt}}_{\delta})$:$\boldsymbol{\sigma}$:$\boldsymbol{\sigma} > 0$. For 2D elasticity, $\boldsymbol{\varepsilon} = (\varepsilon_{11}, \varepsilon_{22}, \varepsilon_{12})^{\text{T}}$ and $\boldsymbol{\sigma} = (\sigma_{11}, \sigma_{22}, \sigma_{12})^{\text{T}}$. From Eq. (2.21) and definitions in Eqs. (3.3) and (3.4), using $\boldsymbol{\varepsilon} = (1,1,0)^{\text{T}}$ and $\boldsymbol{\sigma} = (1,1,0)^{\text{T}}$ gives

$$K^{\text{R}} \equiv (A^{\text{R}})^{-1} < (A^{\text{tt}}_{\delta_0})^{-1} < (A^{\text{tt}}_{n'\delta_0})^{-1} < (A^{\text{tt}}_{n\delta_0})^{-1} < K^{\text{eff}} < K^{\text{dd}}_{n\delta_0} < K^{\text{dd}}_{n'\delta_0} < K^{\text{dd}}_{\delta_0} < K^{\text{V}}, \quad \forall 1 < n' < n \tag{3.5}$$

and using $\boldsymbol{\varepsilon} = (1,-1,0)^{\text{T}}$ and $\boldsymbol{\sigma} = (1,-1,0)^{\text{T}}$ gives

$$\mu^{\text{R}} \equiv (\chi^{\text{R}})^{-1} < (\chi^{\text{tt}}_{\delta_0})^{-1} < (\chi^{\text{tt}}_{n'\delta_0})^{-1} < (\chi^{\text{tt}}_{n\delta_0})^{-1} < \mu^{\text{eff}} < \mu^{\text{dd}}_{n\delta_0} < \mu^{\text{dd}}_{n'\delta_0} < \mu^{\text{dd}}_{\delta_0} < \mu^{\text{V}}, \quad \forall 1 < n' < n \tag{3.6}$$

The difference between K_δ^{dd} and $(A_\delta^{tt})^{-1}$ (or the difference between μ_δ^{dd} and $(\chi_\delta^{tt})^{-1}$) as a function of the window scale δ, can be a measure of the convergence of window size to the RVE size. The difference between K_δ^{app} and K^{eff} (or the difference between μ_δ^{app} and μ^{eff}, app indicates dd or tt) as a function of window scale δ, can be a measure of the decay of anisotropy of apparent property, which also indicates the convergence of apparent properties to the effective ones.

We conduct numerical calculations (by ANSYS 5.4) to verify the above inequalities (3.5) and (3.6) and investigate the convergence of apparent properties to effective ones. In the parametric study, we fix the Poisson's ratios of inclusion and matrix as $\nu^{(i)} = \nu^{(m)} = 0.3$, and vary the ratio between the Young's moduli of both phases (Young's modulus of matrix is assumed to be 1). The volume fraction of fibers is assumed as 35%. The results are given in Tables 1 and 2.

It can be seen that the apparent property under our mixed boundary condition is the same, within numerical accuracy, as the one under periodic boundary condition, which actually gives the effective property. It is bounded by those obtained under displacement and traction boundary conditions. Note that for the second loading case (needed to evaluate μ^{app}), we could alternatively use Eq. (2.3) with $\varepsilon_{11}^0 = \varepsilon_{22}^0 = 0$

Table 1
Apparent bulk modulus K_δ^{app} as a function of stiffness mismatch, boundary conditions and window size

	Traction (tt)	Periodic (pp) or mixed (dt)	Displacement (dd)	Window size
$E^{(i)}/E^{(m)} = 0.001$	0.00643	0.336	0.359	$\delta = \delta_0$
	0.0105		0.347	$\delta = 2\delta_0$
	0.0190		0.345	$\delta = 4\delta_0$
0.1	0.325	0.442	0.461	$\delta = \delta_0$
	0.364		0.452	$\delta = 2\delta_0$
	0.399		0.450	$\delta = 4\delta_0$
10	1.503	1.544	1.864	$\delta = \delta_0$
	1.521		1.682	$\delta = 2\delta_0$
	1.529		1.606	$\delta = 4\delta_0$
1000	1.627	1.681	46.634	$\delta = \delta_0$
	1.653		20.797	$\delta = 2\delta_0$
	1.663		10.691	$\delta = 4\delta_0$

Table 2
Apparent shear modulus μ_δ^{app} as a function of stiffness mismatch, boundary conditions and window size

	Traction (tt)	Periodic (pp) or mixed (dt)	Displacement (dd)	Window size
$E^{(i)}/E^{(m)} = 0.001$	0.00267	0.148	0.173	$\delta = \delta_0$
	0.00623		0.160	$\delta = 2\delta_0$
	0.0139		0.156	$\delta = 4\delta_0$
0.1	0.123	0.187	0.207	$\delta = \delta_0$
	0.152		0.197	$\delta = 2\delta_0$
	0.171		0.194	$\delta = 4\delta_0$
10	0.594	0.642	0.832	$\delta = \delta_0$
	0.620		0.748	$\delta = 2\delta_0$
	0.631		0.699	$\delta = 4\delta_0$
1000	0.640	0.713	25.650	$\delta = \delta_0$
	0.681		14.825	$\delta = 2\delta_0$
	0.698		8.428	$\delta = 4\delta_0$

and $\varepsilon_{12}^0 = 1$. For such a loading, another type of mixed boundary condition, which involves specified tangent displacements and zero normal tractions, would give us the same response as the periodic boundary condition.

As the window size increases, the bounds become tighter, and the differences between apparent properties under different kinds of boundary conditions become smaller. The higher is the mismatch of the phases' properties, the wider are the bounds. For soft inclusion case, the effective property is close to the upper bound, while for stiff inclusion case, it is close to the lower bound. This behavior is further illustrated by Figs. 2 and 3, which show the contour plots of element energy of $\delta = 4\delta_0$ under loading (2). Fig. 2 shows that, for the stiff fiber case, the patterns under periodic and traction boundary conditions are alike, while Fig. 3 shows that, for the soft fiber case, the periodic and displacement boundary conditions patterns are akin.

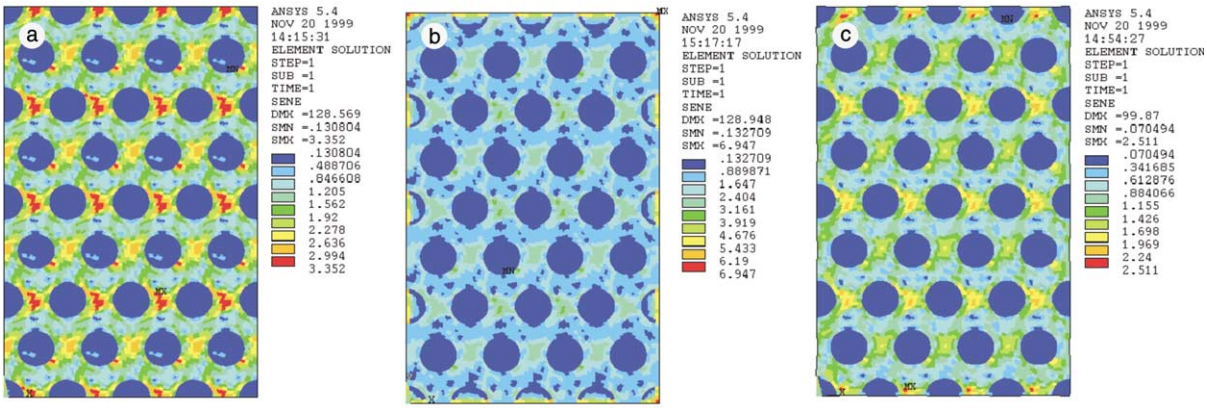

Fig. 2. Contour plots of elastic strain energy when $\delta = 4\delta_0$ and $E^{(i)}/E^{(m)} = 10$ under loading (2): (a) periodic boundary conditions (pp), (b) displacement boundary conditions (dd), (c) traction boundary conditions (tt).

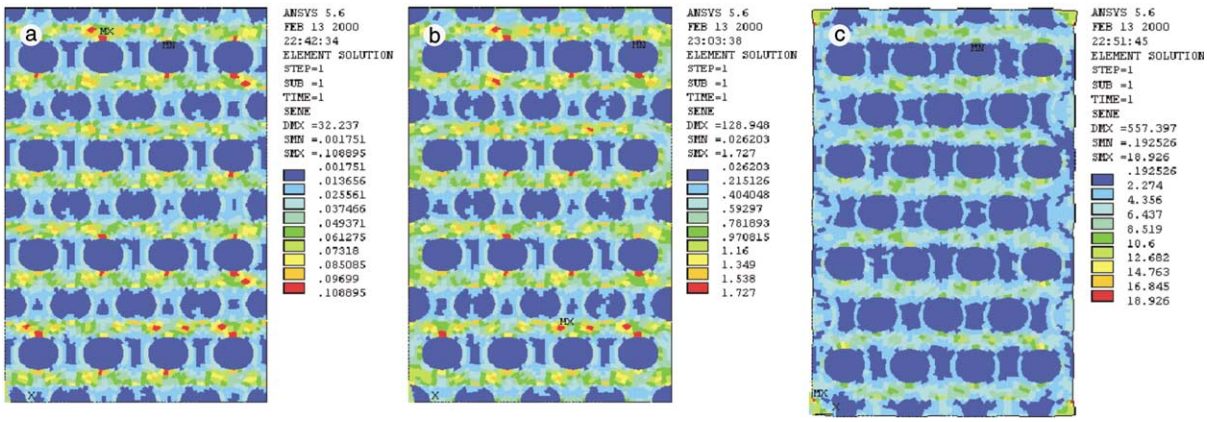

Fig. 3. Contour plots of elastic strain energy when $\delta = 4\delta_0$ and $E^{(i)}/E^{(m)} = 0.1$ under loading (2): (a) periodic boundary conditions (pp), (b) displacement boundary conditions (dd), (c) traction boundary conditions (tt).

4. Apparent elastoplastic responses

In this section, we study the elastoplastic behavior of metal–matrix composites (MMC) as an example of general nonlinear composites. The MMC considered here consists of elastoplastic isotropic matrix reinforced with linearly elastic, isotropic fibers. The volume fraction of fibers is 35% as before.

From the study of apparent elastic properties in the last section we already found that there is a big difference between the apparent properties obtained under various boundary conditions if there is a significant mismatch between the properties of fibers and matrix. In order to quantify the mechanical response during plastic deformation, we consider a special metal–matrix composite, in which elastic properties of matrix and fibers are the same. For the matrix, the von Mises yield criterion is used, and the rate-independent plasticity with associated flow rule and isotropic hardening is assumed. The matrix' stress–strain curve is characterized by a piecewise power law

$$\frac{\sigma}{\sigma_0} = \begin{cases} \varepsilon/\varepsilon_0, & \text{if } \varepsilon \leqslant \varepsilon_0 \\ (\varepsilon/\varepsilon_0)^N, & \text{else} \end{cases} \tag{4.1}$$

with yield stress $\sigma_0 = E\varepsilon_0$, where E is Young's modulus and ε_0 is yield strain.

In the elastic range (prior to yielding) our material is homogeneous with the stress and strain being uniform, and its elastic response is independent of the boundary conditions. We choose the same elastic properties of matrix and fibers on purpose so that we can directly study the effect of coupled scale and boundary conditions effects for plastic material response.

In numerical calculations we apply loading (2) discussed in Section 3. For clarity, we restate the loadings under all the boundary conditions: (i) Under displacement and periodic boundary conditions, the prescribed strains are $\varepsilon^0_{11} = -\varepsilon^0_{22} = \varepsilon^0$, $\varepsilon^0_{12} = 0$. (ii) Under traction boundary condition, the prescribed stresses are $\sigma^0_{11} = -\sigma^0_{22} = \sigma^0$, $\sigma^0_{12} = 0$. (iii) Under mixed boundary condition, the prescribed strains are $\varepsilon^0_{11} = -\varepsilon^0_{22} = \varepsilon^0$, and the prescribed stress is $\sigma^0_{12} = 0$.

The material constants used in our calculations (Eq. (4.1)) are $\varepsilon_0 = 1/300$, $\sigma_0 = 170$ MPa, $N = 0.1$, $E = \sigma_0/\varepsilon_0 = 51$ GPa, $v = 0.3$. The computation is done by the FEA software ABAQUS 5.5 (Hibbit, Karlson, Sorensen, Inc., , 1995). Two window sizes are considered: δ_0 and $4\delta_0$.

In Figs. 4 and 5, we show the equivalent plastic strain (PEEQ) contour plots under different boundary conditions, when $\delta = \delta_0$ and $\delta = 4\delta_0$, respectively. The equivalent (effective) strain is defined in Eq. $(2.13)_2$. In all the contour plots, under displacement (Figs. 4c and 5c), mixed (Figs. 4b and 5b), and periodic (Figs. 4a and 5a) boundary conditions, we show the equivalent plastic strain (PEEQ) when applied strain in the x_1-direction is 15 times the yield strain ε_0, while under traction boundary conditions (Figs. 4d and 5d) we show the PEEQ when applied stress in the x_1-direction is the same as the yield stress σ_0.

Under displacement boundary conditions at $\delta = \delta_0$ (Fig. 4c), it is observed that there are two kinds of shear bands formed, one around the fibers at the corners and one along the lines having angles of $\pi/3$ and $2\pi/3$ with respect to the x_1-direction. The largest plastic deformation occurs in the interior of the unit cells and close to the interfaces between matrix and fibers. There are regions in the matrix with only elastic deformation. This is why the composite under displacement boundary conditions is stronger than the composite under other conditions, whose shear band characteristic will be discussed below. Under traction boundary conditions (Fig. 4d), the dominant shear bands are oriented at $\pi/4$ and go through the matrix in unit cells. The largest plastic deformation is not at the interface between fiber and matrix, but is located near the centers of top and bottom boundaries of a window. The shear band patterns under periodic and mixed boundary conditions (Fig. 4a and b) are very similar to each other. In both cases, the shear bands are distributed uniformly in the matrix, and there is no dominant shear band crossing the matrix. The shear band patterns under traction, periodic and mixed boundary conditions give the explanation of character of the associated stress–strain curves given in Fig. 6, showing that the elastoplastic behavior under traction boundary conditions is softer than those under periodic and mixed conditions. The responses under the

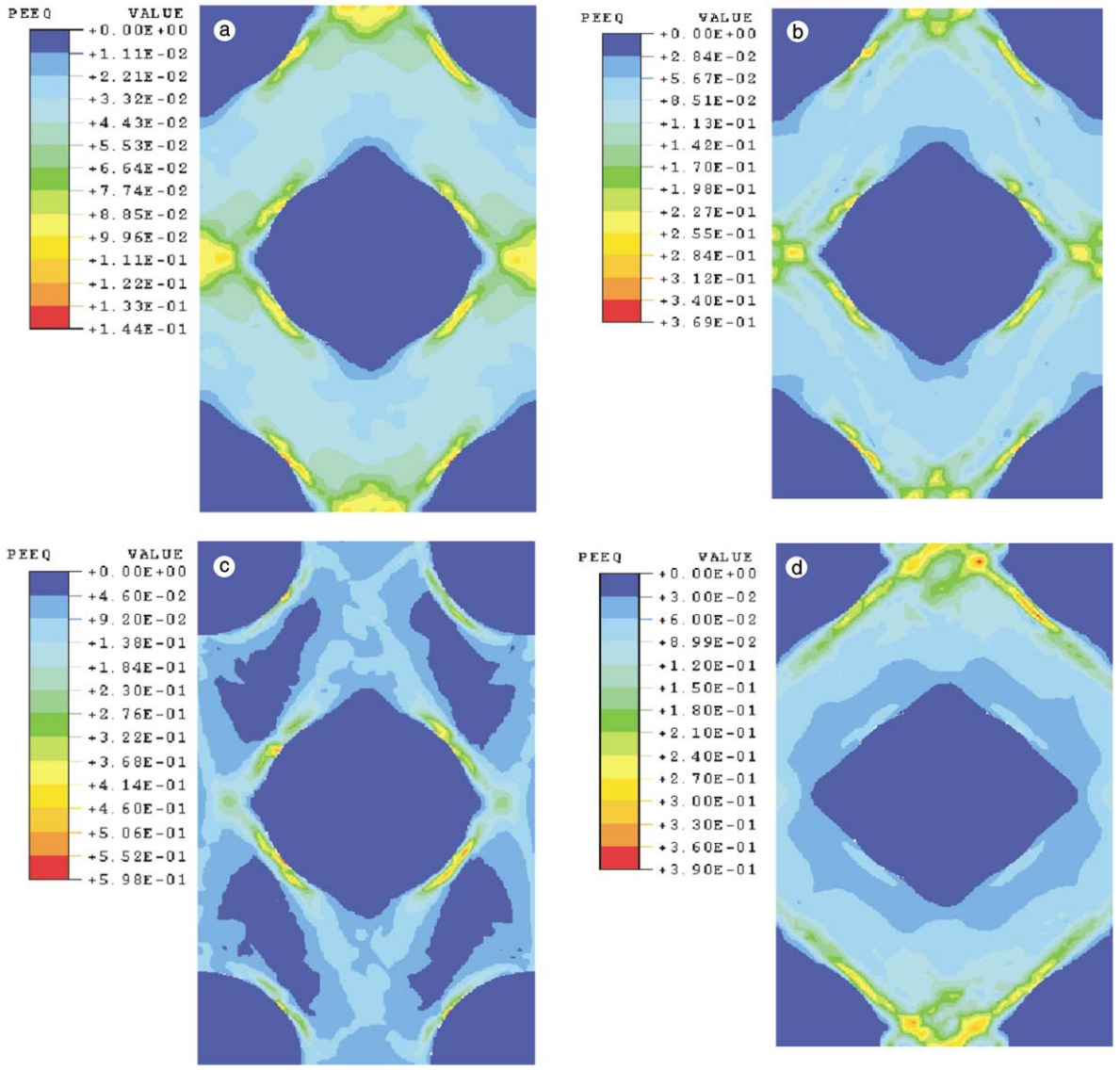

Fig. 4. Contour plots of equivalent plastic strain (PEEQ) when $\delta = \delta_0$: (a) periodic boundary conditions (pp), (b) mixed boundary conditions (dt), (c) displacement boundary conditions (dd), (d) traction boundary conditions (tt).

latter two conditions are identical within numerical error. The similarity between the elastic (see last section) and elastoplastic responses under mixed and periodic boundary conditions can be expected because under periodic conditions, the deformation of unit cells adjacent should be symmetric about the common boundary. This means the boundaries of a unit cell under periodic boundary conditions should be shear stress free, which is, in fact, required in our mixed boundary condition under the loading considered.

When the window size increases ($\delta = 4\delta_0$), from Fig. 5 we see similar trends to those at $\delta = \delta_0$, but the differences between the PEEQ patterns under different boundary conditions become smaller. However,

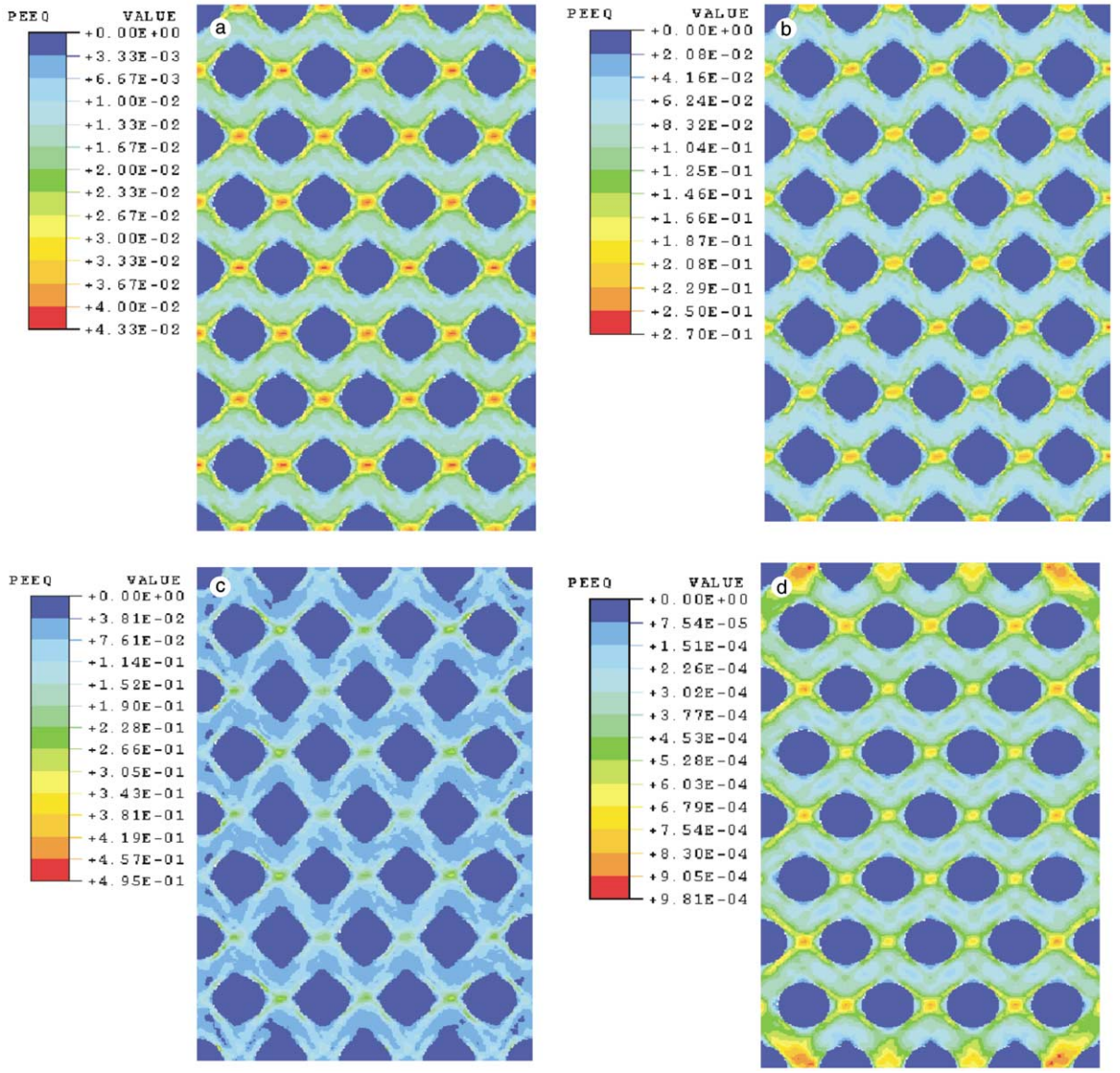

Fig. 5. Contour plots of equivalent plastic strain (PEEQ) when $\delta = 4\delta_0$: (a) periodic boundary conditions (pp), (b) mixed boundary conditions (dt), (c) displacement boundary conditions (dd), (d) traction boundary conditions (tt).

under traction boundary conditions (Fig. 5b), we still observe more plastic deformation concentrated at the window edges, compared to the ones under other boundary conditions.

In Fig. 6, we plot the response curves (averaging stress–strain relationship in x_1-direction) under different boundary conditions when $\delta = \delta_0$ and $\delta = 4\delta_0$. It shows that, as the window size increases, bounds become tighter, and they are closer to the effective response curve. We also see that the response under the particular mixed boundary condition, considered in this paper, does not depend on the window size, and it is almost the same as the effective response obtained under periodic boundary condition.

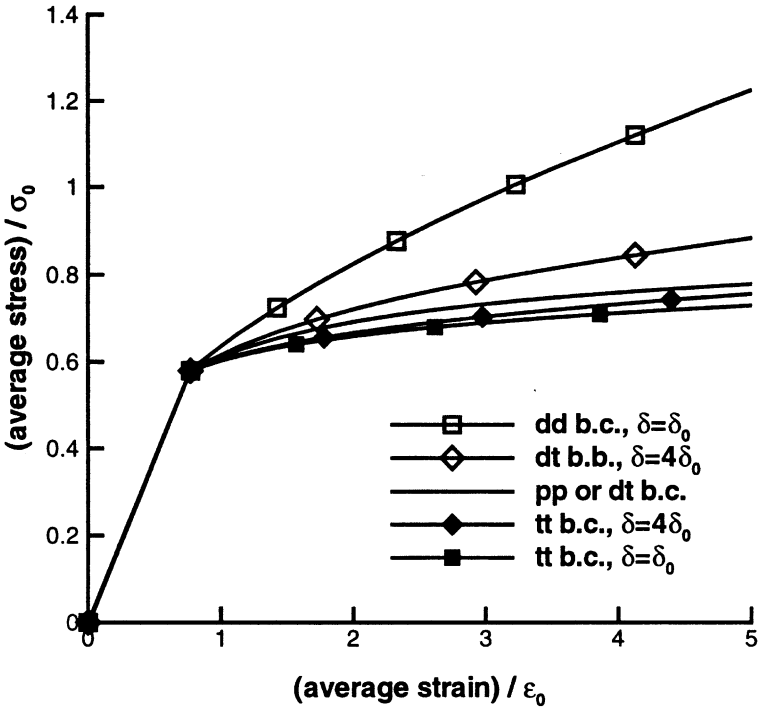

Fig. 6. Elastoplastic stress–strain responses under different boundary conditions.

Our paper (Jiang et al., 2001a) gave results on coupled scale and boundary conditions effects valid for any elastoplastic hardening material. They were derived for microstructures of arbitrary spatially homogeneous and ergodic statistics. In this paper we illustrate it for a composite with a periodic microstructure, a particular type of strict-sense, cyclo-stationary statistics. We chose an elastoplastic law of Ramberg–Osgood type for simplicity, and provided numerical results for one choice of parameters. Other specific constitutive laws, as well as other selections of parameters, could be implemented, but no extra generality of qualitative behaviors would be accomplished. More specifically, the effective elastoplastic response would be bounded from above and below by the apparent ones obtained from displacement and traction boundary conditions, and these bounds would become tighter for larger window sizes. Further parametric studies can be done in the future.

5. Concluding remarks

We investigated the scale and boundary conditions effects on the elastic and elastoplastic responses of periodic (triangular packing) 2D composites. Even though the effective properties are isotropic, the apparent ones under displacement and traction controlled boundary conditions are orthotropic. It is shown that the apparent elastic and elastoplastic properties obtained under mixed and periodic conditions are the same within numerical accuracy, and they are bounded by properties obtained using displacement and traction controlled boundary conditions. This result tells us that for a periodic composite, one can use the smallest window, a unit cell, subject to our special mixed boundary condition (normal displacements and

zero shear tractions specified on each boundary) for the two loadings considered, to obtain the effective response, by either numerical simulation or real experiment.

In addition, we find that bounds on effective elastic moduli are very sensitive to the mismatch of phase moduli: the higher the mismatch, the wider the bounds. As the window size increases, the difference between the responses under different boundary conditions becomes smaller.

Our elastoplasticity study showed that the stress–strain curves under periodic boundary conditions (i.e., effective stress–strain) curves are bounded, respectively from above and below, by responses under displacement and traction boundary conditions, and, as the window size increases, the bounds become tighter.

This investigation provides a framework for studying composites with random fiber arrangements. For non-periodic composites, we cannot use periodic boundary conditions. Thus the issue of the choice of boundary condition and window size becomes important. This subject was studied in (Jiang et al., 2001b) in the context of out-of-plane elasticity and in (Jiang et al., 2001a) in the context of in-plane elastoplasticity of random composites.

Finally, the focus of this paper is on "computational experiments" which allow us to predict effective and apparent properties of composite materials numerically. The following issues guided us not to include experiments:

- pure displacement and traction conditions are very difficult to realize in the laboratory;
- boundary conditions usually employed in experiments are of certain mixed type where tractions are applied on one part of the boundary, and displacements on the other; the mixed boundary conditions considered in this paper are of special type where one component of traction and another one of displacement is specified on the entire boundary; similar boundary conditions were applied experimentally by Papka and Kyriakides (1999).

Acknowledgements

Support by the NSF under grants CMS-9713764 and CMS-9753075 is gratefully acknowledged. We benefited from comments of an anonymous reviewer.

References

Accorsi, M.L., Nemat-Nasser, S., 1986. Bounds on the overall elastic and instantaneous elastoplastic moduli of periodic composite. Mech. Mater. 5, 209–220.

Brockenbrough, J.R., Suresh, S., Wienecke, H.A., 1991. Deformation of metal-matrix composites with continuous fibers: geometrical effects of fiber distribution and shape. Acta Metall. Mater. 39, 735–752.

Gibiansky, L., Torquato, S., 1998. Effective energy of nonlinear elastic and conducting composites: approximations and cross-property bounds. J. Appl. Phys. 84, 5969–5976.

Hazanov, S., 1998. Hill condition and overall properties of composites. Arch. Appl. Mech. 68, 385–394.

Hazanov, S., 1999. On apparent properties of nonlinear heterogeneous bodies smaller than the representative volume. Acta Mech. 134, 123–134.

Hazanov, S., Amieur, M., 1995. On overall properties of elastic heterogeneous bodies smaller than the representative volume. Int. J. Engng. Sci. 23, 1289–1301.

Hazanov, S., Huet, C., 1994. Order relationships for boundary conditions effect in heterogeneous bodies smaller than representative volume. J. Mech. Phys. Solids 42, 1995–2011.

Hibbit, Karlson, Sorensen, Inc., 1995. 1080 Main Street, Pawtucket, RI, USA, ABAQUS User's Manual version. 5.5.

Hollister, S.J., Kikuchi, N., 1992. A comparison of homogenization and standard mechanics analyses for periodic porous composites. Comput. Mech. 10, 73–95.

Huet, C., 1990. Application of variational concepts to size effects in elastic heterogeneous bodies. J. Mech. Phys. Solids 38, 813–841.

Jiang, M., Ostoja-Starzewski, M., Jasiuk, I., 2001a. Scale-dependent bounds on effective elastoplastic response of random composites. J. Mech. Phys. Solids 49 (3), 655–673.

Jiang, M., Alzebdeh, K., Jasiuk, I., Ostoja-Starzewski, M., 2001b. Scale and boundary conditions effects in elasticity of random composites. Acta Mech. 148, 63–78.

Kröner, E., 1994. Nonlinear elastic properties of micro-heterogeneous media. ASME J. Engng. Mat. Technol. 11, 325–330.

Ostoja-Starzewski, M., 1993. Micromechanics as a basis of random elastic continuum approximations. Prob. Engng. Mech. 8, 107–114.

Ostoja-Starzewski, M., 1998. Random field models of heterogeneous materials. Int. J. Solids Struct 35, 2429–2455.

Ostoja-Starzewski, M., 1999. Scale effects in materials with random distributions of needles and cracks. Mech. Mater. 31, 883–893.

Papka, S.D., Kyriakides, S., 1999. In-plane biaxial crushing of honeycombs: Part I Experiments. Int. J. Solids Struct 36, 4367–4396.

Pecullan, S., Gibiansky, L.V., Torquato, S., 1999. Scale effects on the elastic behaviour of periodic and hierarchical two-dimensional composites, J. Mech. Phys. Solids 47, 1509–1542.

Castañeda, P.P., 1992. New variational principles in plasticity and their application to composite materials. J. Mech. Phys. Solids 40, 1757–1788.

Castañeda, P.P., Suquet, P., 1998. Nonlinear composites. Adv. Appl. Mech. 34, 171–302.

Shen, Y., Finot, M., Needleman, A., Suresh, S., 1995. Effective plastic response of two-phase composites. Acta Metall. Mater. 43, 1701–1722.

Talbot, D.R.S., Willis, J.R., 1985. Variational principles for inhomogeneous non-linear media. IMA J. Appl. Math. 35, 39–54.

Talbot, D.R.S., Willis, J.R., 1998. Upper and lower bounds for the overall response of an elastoplastic composite. Mech. Mater. 28, 1–8.

Werwer, M., Cornec, A., Schwalbe, K.-H., 1998. Local strain fields and global plastic response of continuous fiber reinforced metal-matrix composites under transverse loading. Comput. Mater. Sci. 12, 124–136.